X-ray diffraction on $(KBr)_{1-x}(KCN)_x$ mixed crystals

K. Knorr and A. Loidl
Institut für Physik, Universität Mainz, 6500 Mainz, Federal Republic of Germany
(Received 6 August 1984; revised manuscript received 26 October 1984)

X-ray powder diffraction experiments have been carried out on eight mixed crystals ($x=0.20$, 0.50, 0.53, 0.65, 0.70, 0.80, 0.85, and 0.90) in the temperature range from 15—300 K. The phase diagram shows cubic, rhombohedral, monoclinic, and triclinic phases, and a glass state. The structural order parameters and the width of the cubic powder lines have been studied in detail as a function of temperature. The character of the transition from the cubic to the low-temperature phases changes from strongly discontinuous for $x=0.9$ to quasicontinuous for $x=0.65$. The glass state can be described by distributions of shear strains.

INTRODUCTION

The alkalicyanides show a rich variety of structural effects[1] which are interpreted in terms of an interaction of the orientational degrees of freedom of the aspherical CN^- molecules with the lattice strains. The most rigorous theoretical treatment of this type was given recently by Michel.[2]

Below the melting temperature the mixed crystals $(KBr)_{1-x}(KCN)_x$ crystallize in the rocksalt structure, the CN^- molecules being rotationally disordered. The probability distribution of their orientations can be described in terms of cubic harmonics with maxima along $\langle 111 \rangle$.[3] For higher CN concentrations a transition to a low-temperature state of orientational order accompanied by changes of the translation symmetry of the center-of-mass lattice has been observed. The transitions are announced by a softening of the elastic constants, particularly the T_{2g} constant, C_{44}.[4,5] Until recently it was tacitly assumed that the low-temperature phase of the mixed crystals is identical to the orthorhombic low-temperature phase of pure KCN, but Rowe *et al.*[6] demonstrated that for CN concentrations of $x=0.80$ the low-temperature phase is actually monoclinic. For $x=0.90$ and 0.95 they observed a coexistence of orthorhombic and monoclinic structures. In Br-rich mixed crystals ($x<0.56$) anomalies of the electric and strain susceptibilities, as measured by dielectric-,[7,8] ultrasonic-,[9] and inelastic-neutron-scattering experiments[10,11] have been taken as indications of a freezing of the CN systems into glasslike orientational patterns.

A tentative phase diagram, which already contains the information which will be brought forth in the present article, is shown in Fig. 1. It bears a great resemblance to the phase diagrams of diluted magnetic systems, in which one identifies the following magnetic states: paramagnetic, ferromagnetic, and spin glass with the states orientationally disordered cubic, orientationally ordered noncubic, and orientational glass. In magnetic systems there is usually one unique type of magnetic long-range order, e.g., ferromagnetism, whereas in the present case several ordered phases exist.

We will present x-ray-diffraction results on samples with eight different CN concentrations ($x=0.20$, 0.50, 0.53, 0.65, 0.70, 0.80, 0.85, and 0.90).

EXPERIMENTAL DETAILS

The single crystal of $(KBr)_{1-x}(KCN)_x$ were grown from the melt employing the Czochralski technique. Two samples were purchased from the crystal-growth laboratory of the University of Utah; the others were kindly supplied by S. Haussühl of the University of Köln. The concentrations were determined gravimetrically, and the error in x is 0.03. Powders of 10—50 μm grain size were prepared by grinding. The powder was sprayed onto a Si(100) wafer and held in place by soaking it with a small amount of molten vacuum grease. The platelet was attached to the cold plate of a closed-cycle refrigerator, which is equipped with a Be cylinder for allowing the passage of the x rays. Two Si diodes were used as thermometers, one directly on the cold plate and the other on the Si wafer. The temperature was stabilized by a controller to better than 0.03 K.

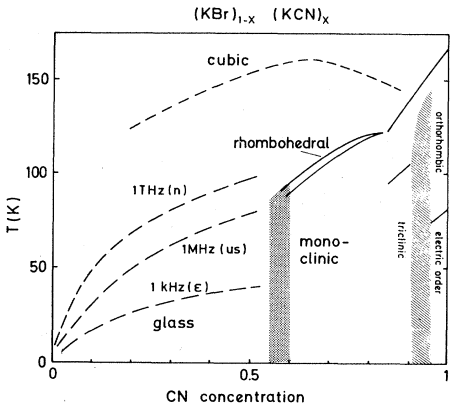

FIG. 1. Approximate phase diagram for $(KBr)_{1-x}(KCN)_n$. Phase boundaries are shown as solid lines, the frequency dependent freezing temperature as dashed lines. The hatched area is a coexistence region, the dotted one the transition region from elastic ordering to the glass state.

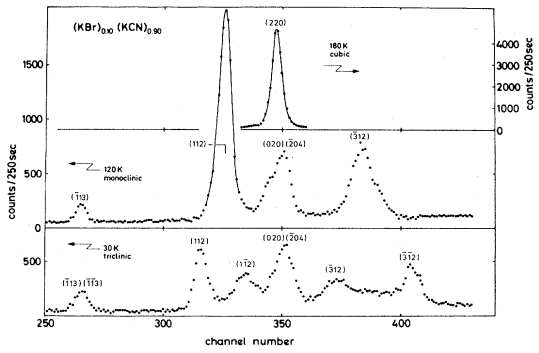

FIG. 2. Parts of powder spectra on $(KBr)_{0.9}(KCN)_{0.1}$ showing the splitting of the cubic (220) powder line and the appearance of the extra line, $(\bar{1}13)$, in the low-temperature phases.

The x rays emerged from a Cu x-ray tube operated at 40 kV and 20 mA. A graphite monochromator was set to reflect the $K\alpha$ component (1.542 Å). The powder spectrum was measured by means of a flat, position-sensitive detector. In the geometry chosen the detector spanned an arc of 20° in the scattering angle 2θ. Usually, a sample was investigated with the detector in two different positions. The diffraction patterns will be presented as x-ray counts versus channel number, where the channel number is a linear measure of the position along the detector. No attempt was made to calibrate the spectra in absolute scattering angles, but rather a relative calibration was used wherein the cubic reflections were taken as reference. Roughly an increment of plus one channel corresponds to an increment of $+0.046°$ in 2θ. More exact nonlinear relations, specific to the particular setup, were used in the analysis of the data.

Figure 2 shows a typical result obtained in a counting time of 250 sec. The section shown is the vicinity of the cubic (220) Debye-Scherrer line at about $2\theta=39°$. The intrinsic spatial resolution of the detector is about two channels. The actual resolution is larger due to the $K\alpha_1$-$K\alpha_2$ doublet, the vertical divergence of the beam, the rough surface of the sample, and the fact that the detector coincides with the focusing circle at one point only.

In the present context it is important to recall two basic facts of x-ray diffraction. First, the contribution of the light elements C and N to the scattering in the presence of K and Br is almost negligible. In particular, there is no chance to derive direct information on the CN orientations, although under the action of a bilinear coupling of rotations and translations, changes of the orientations will show up in the K and Br translational correlations. Second, an x-ray-diffraction experiment cannot distinguish between static and dynamic structures. Thus one should regard the Debye-Scherrer diagrams as snapshots of the center-of-mass arrangements.

RESULTS

In the powder spectra of the mixed crystals, cubic, rhombohedral, monoclinic, and triclinic patterns were observed.

Monoclinic phases

The samples with concentrations ranging from $x=0.65$ to 0.90 show a cubic-to-monoclinic structural phase transition which is observable through the splitting of the fcc reflections and the appearance of additional reflections below the ordering temperature. The splitting of the cubic (220) powder line into the monoclinic (112), (020), $(\bar{2}04)$, and $(\bar{3}12)$ lines is shown in Figs. 2 and 3. Here, the monoclinic reflections are indexed in terms of the cell of Ref. 6 and are listed with increasing scattering angle. The two inner lines could not be resolved, except for $x=0.80$ and some temperatures for $x=0.90$. The critical temperature T_c, the overall splitting, and the jump of the splitting at T_c increase monotonically with CN concentration. The onset of the monoclinic phase for $x=0.80$, 0.85, and 0.90 is discontinuous; for $x=0.65$ and 0.70 we observed more continuous and more complicated changes of the diffraction patterns around T_c; these will be discussed later. The transitions of the three samples with high CN concentrations exhibit hysteresis effects on the order of 2 K upon cooling and heating. The parameters of the monoclinic cells—a, b, c, and β—were derived from the position of the lines. Reference to the cubic phase (lattice constant a_c) is made in terms of the increments ϵ, Δ, δ, and ϕ as defined in Fig. 4. One notes from this figure that the cubic-to-monoclinic distortion can be mainly described by a change of the monoclinic a axis, which shrinks relative to the cubic structure and tips over toward the cubic [011] direction. The changes of the other two axes are smaller by 1 order of magnitude. An alternative description of the changes of the cell can be given in the following way, where the data of the highest temperature of the monoclinic phase are compared to those of the cubic phase, and the values are given for decreasing CN concentration ($x=0.9$, 0.85, 0.60, 0.70, and

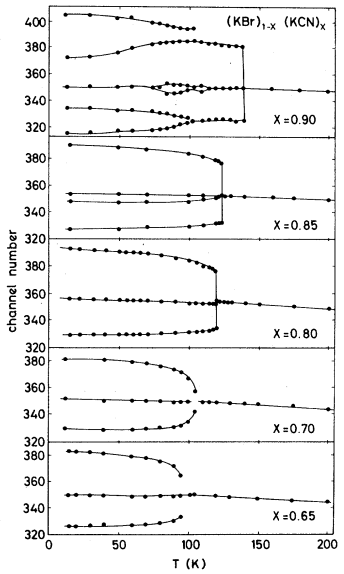

FIG. 3. Temperature dependence of the positions of the powder lines of monoclinic and triclinic phases resulting from the cubic (220) line.

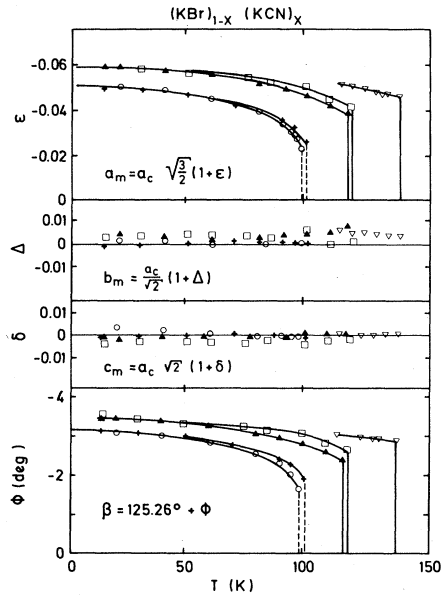

FIG. 4. Order parameters of the monoclinic phase as a function of temperature. The monoclinic cell parameters a_m, b_m, c_m, and β are related to the cubic cell (lattice constant a_c) in terms of the relative increments ϵ, Δ, and δ, and the change ϕ of the cell angle.

0.65). The cell volume is compressed (A_{1g} compression) by 0.6%, 0.3%, 0%, 0%, and 0.25%, one of the former cubic axes, say the b axis, is compressed (e_g strains) relative to the other two by 0.83%, 0.78%, 0.82%, 0.15%, and 0.16%, and the angles α and γ are reduced by 3.22°, 2.95°, 2.65°, 2.13°, and 1.83°, whereas β remains at 90°.

In the monoclinic phase, reflections have been detected which are related to the L points of the original cubic Brillouin zone. The integrated intensity of one of these lines, $(\bar{1}13)$, is shown as a function of temperature in Fig. 5. Again, one notes a change from a discontinuous onset

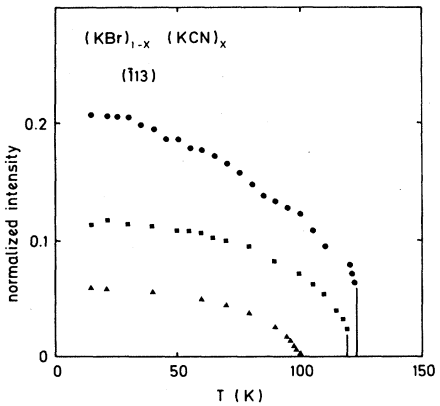

FIG. 5. Temperature dependence of the integrated intensity of the $(\bar{1}13)$ line of the monoclinic lattice. The intensities are normalized to the integrated intensity of the cubic (220) line just above the transition temperature. ●, $x=0.85$; ■, $x=0.80$; ▲, $x=0.65$.

for higher CN concentrations to a continuous one at lower CN concentrations. The intensity of these lines is connected to a plus-minus staggering of the internal displacements with respect to the cubic positions that propagates through the lattice with a wave vector $(\frac{1}{2},\frac{1}{2},\frac{1}{2})$ in cubic notation. The atomic positions of the monoclinic phase for $x=0.95$, 0.90, and 0.80 have been, in fact, determined by Rowe *et al.*[6] from neutron powder diffraction data. The space group was identified as C_s^4.

Triclinic phase

As can be seen from Fig. 3, the monoclinic phase of the sample with $x=0.9$ is stable between 140 and 105 K. Below 105 K one observes a further splitting of the monoclinic lines due to a lifting of the degeneracy of the monoclinic-line position with respect to $\pm k$; hence, a triclinic deformation, occurs as is illustrated in Figs. 2 and 3 for the monoclinic lines (1 ± 12) and $(\bar{3}\pm12)$. In the triclinic phase the parameters $-\phi$ and $-\epsilon$ from above increase by another 10%. The cell parameters α and γ, which were 90° in the monoclinic phase, change at 105 K discontinuously by $-0.2°$ and 0.4°, increase with decreasing temperature, and finally reach low-temperature values of 90°−0.7° and 90°+2.32°. As for the other samples, several cooling and heating cycles were performed, and, occasionally, mainly at higher temperatures, weak lines appeared that were not consistent with the monoclinic and triclinic lattices; in most cases they occurred at those scattering angles where one expects strong reflections from an orthorhombic phase, which, according to Rowe *et al.*,[6] coexists with a monoclinic phase at $x=0.90$. In any case, the line $x=0.90$ in the phase diagram seems to be close to, or may even intersect, a phase boundary. From our measurements the coexistence at low temperatures should be triclinic-orthorhombic rather than monoclinic-orthorhombic.

Intermediate rhombohedral phase

As mentioned above, the samples with $x=0.70$ and 0.65 show a more complex diffraction pattern in the vicinity of the cubic-to-monoclinic transition temperature T_c. There exists a small temperature interval of about 3 K where the cubic lines split into a lower number of peaks than expected in a monoclinic structure. There is, e.g., no splitting of the (400) line, and the (440) line splits into two rather than three peaks. Examples of raw diffraction data for scattering angles around the cubic (220) line are reproduced in Figs. 6 and 7. The peak positions derived from these figures are shown in Fig. 8. These results suggest an intermediate rhombohedral phase where the rhombohedral distortion develops continuously. The maximum distortion is reached at 104 K for $x=0.70$ and 97 K for $x=0.65$. Here, the cell angles are sheared by $+1.1°$ in either case, whereas the lattice constant is unchanged with respect to the cubic cell just above the transition.

Despite the fact that the two samples share the same shear magnitude, there are clear differences between them. For $x=0.70$ the subsequent rhombohedral-to-monoclinic transition is continuous, whereas it is discontinuous for $x=0.65$ with a coexistence of rhombohedral and mono-

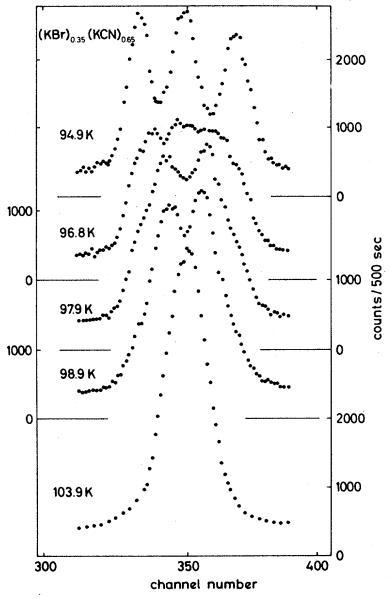

FIG. 6. Parts of powder spectra for $x=0.65$ showing the splitting of the cubic (220) line.

clinic diffraction patterns, as indicated in Fig. 8. Superlattice lines have not been observed in the intermediate phase.

Linewidth

All samples, with the exception of the one with $x=0.90$ and pure KBr, show a systematic broadening of most of the cubic powder lines that becomes apparent

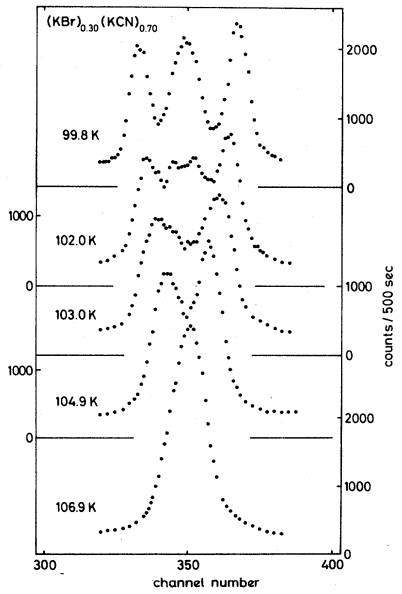

FIG. 7. Parts of the powder spectra for $x=0.70$ showing the splitting of the cubic (220) line.

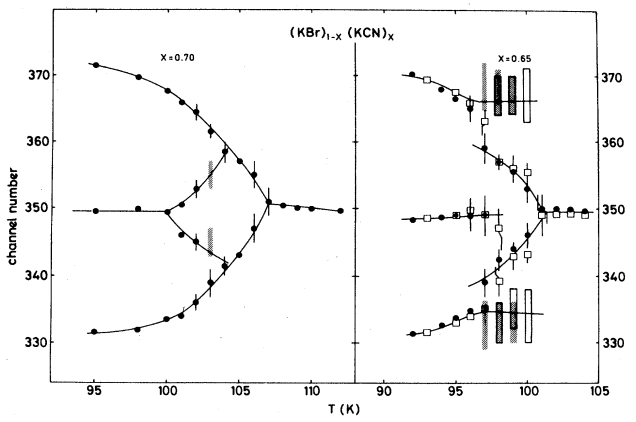

FIG. 8. Temperature dependence of the positions of the powder lines resulting from the cubic (220) line. The open symbols refer to a heating cycle, the closed ones to a cooling cycle.

below a temperature of the order of 150 K (Fig. 9). For the samples showing an ordered low-temperature state ($x \geq 0.65$), the broadening increases when approaching the transition temperature and is either interrupted by the discontinuous onset of the monoclinic splitting ($x=0.80$ and 0.85), or it merges into the continuous evolution of the rhombohedral splitting, as illustrated in Fig. 10 for $x=0.65$. In the nonordering samples ($x=0.53$, 0.50, and 0.20) the broadening finally saturates at the lowest temperatures.

The study of the width of several powder lines revealed that the broadening has T_{2g} symmetry, or, expressed in an alternative way, the lines that broaden most would show the strongest splitting for a cubic-to-rhombohedral phase transition. An example for this anisotropic effect is given in Fig. 11. Note that the (400) width shows no temperature effect, whereas the other two lines are clearly broader at the lower temperature.

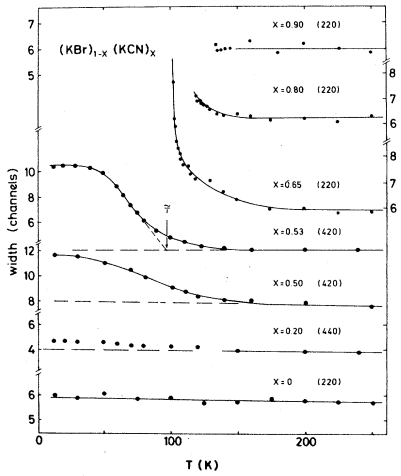

FIG. 9. Apparent width of selected powder lines as a function of temperature.

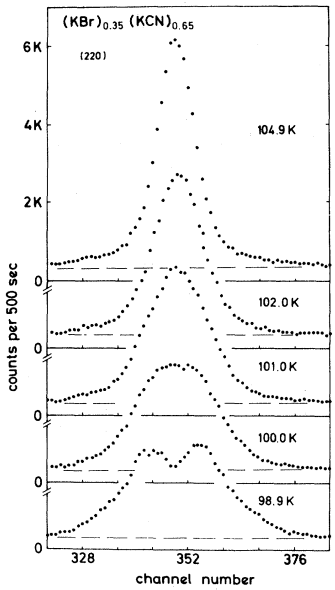

FIG. 10. Parts of powder spectra for $x=0.65$ showing the broadening and splitting of the cubic (220) line in the vicinity of the cubic-to-rhombohedral phase transition.

DISCUSSION

The present results supply additional information on the x,T phase diagram of $(KBr)_{1-x}(KCN)_x$ at ambient pressure. In all, there are four elastically ordered phases (Fig. 1), of which the monoclinic one has the largest existence region. From the work of Rowe *et al.*,[6] it is likely that additional electric ordering of the CN molecules occurs only in the orthorhombic phase. Ignoring those lines of the monoclinic and triclinic phases for the moment, which are related to the L points of the original cubic Brillouin zones, the lattices of the four elastically ordered phases can be understood by ferroelastic deformations of the cubic lattice. In all four cases the A_{1g} and E_g deformations are of secondary importance, and the dominant part of the ferroelastic order parameter ψ are the T_{2g} shears; hence, ψ can be approximately written as a T_{2g} tensor with the elements ϵ_{xy}, ϵ_{yz}, and ϵ_{zx}. In the rhombohedral phase all three elements are equal, in the triclinic phase all three elements are different, and in the monoclinic phase two are equal while the third is zero, whereas in the orthorhombic phase of pure KCN two of them are zero. Thus, all interesting combinations are realized in the system.

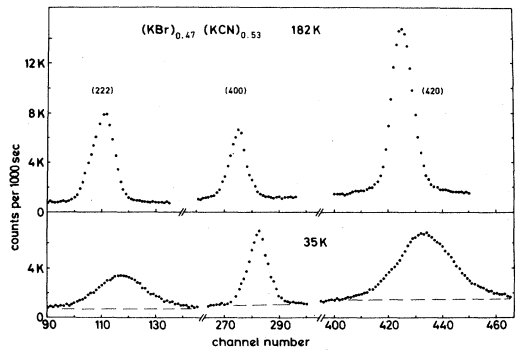

FIG. 11. Three powder lines for $x=0.53$ at 182 and 35 K.

The observations are in qualitative agreement with the results of mean-field calculations, which start from a bilinear coupling between the translations and rotations. Quantitative results have been obtained for special assumptions of the single-ion crystal field and the ψ tensor. According to De Raedt *et al.*,[12] the ferroelastic shear transition is, in general, of first order. The relation between the elements $\epsilon_{\alpha\beta}$ was left undetermined. The jump of the order parameter at T_c can be controlled to some extent by the strength of the crystal field. The antiferrodistortive component of the monoclinic and triclinic phases is not explained by this theory. It is, in fact, difficult to image a strong elastic response at the L point, where (at least for $x=1$) the bilinear rotational-translation coupling should vanish.

Another puzzle is the existence and continuous evolution of the intermediate rhombohedral phase. Generally, a first-order transition from a high- to a low-temperature phase is expected to mask an intermediate phase of such a small width. Thus the appearance of the rhombohedral phase depends on the fact that at least one of the cubic-to-rhombohedral-to-monoclinic transitions is close to second order. The assumption of a continuous cubic-to-rhombohedral transition is somewhat problematic since there exists the third-order invariant $\epsilon_{xy}\epsilon_{yz}\epsilon_{zx}$ in the Landau free energy. The rhombohedral distortion may nevertheless set in continuously since the order parameter is a tensor, as pointed out in Ref. 12, apart from the possibility of a fluctuation-dominated transition.[13] A continuous transition would be connected with a complete softening of the C_{44} phonon modes. As the wave vectors of these modes cover a two-dimensional section of reciprocal space, it was argued that the mean-square displacement $\langle u^2 \rangle$ should diverge at T_c.[14] We will comment on this point later.

The present experiment provides strong evidence for a continuous transition. We recall the most important results: (1) the cubic powder lines broaden when approaching the transition, a fact which is most naturally explained by thermal diffuse scattering from soft C_{44} phonon modes, (2) the rhombohedral splitting evolves from these broadened patterns, and (3) sockets of diffuse scattering exist even at temperatures where the splitting is clearly resolved.

Turning to the line broadening in the nonordering compounds ($x \leq 0.53$), one can assume that the contribution of the thermal diffuse scattering closely follows the temperature dependence of the elastic constants. It should be strongest at the freezing temperature where the elastic constants pass through a minimum. The linewidth at low temperatures must be of a different origin, namely static effects such as finite-size effects, inhomogeneous shear strains, or random-walk patterns of bond angles. The present results cannot distinguish between these possibilities. Following the second possibility, the line shapes can be translated into a distribution of T_{2g} shear strains, cen-

tered around zero strain, and the width can be directly interpreted as the mean-random-field order parameter of the glass state. At low temperatures one arrives at the following values of $(\langle\epsilon_{\alpha\beta}^2\rangle)^{1/2}$: 0.48°, 0.27°, and 0.02° for $x=0.53$, 0.50, and 0.20, respectively. These values do not scale with the x dependence of the freezing temperature (see Fig. 1), but rather decrease rapidly with increasing (x_c-x), where x_c is the lowest concentration of long-range elastic order.

The determination of the freezing temperature $\tilde{T}$ from the experimental data causes some problems. For the compound with $x=0.53$, Fig. 9 shows a very suggestive geometrical construction for $\tilde{T}$. Here, the temperature dependence of the width, in general, and the value of $\tilde{T}$ (about 95 K), in particular, are in good agreement with analogous results of Rowe *et al.*[15] obtained by neutron scattering on a sample, the concentration of which was cited as $x=0.5$. Unfortunately, the geometrical construction is not applicable to the two other nonordering samples. The sample with $x=0.53$ is presumably not representative for the glass state of $(KBr)_{1-x}(KCN)_x$ since it is close to the boundary of the ordered phases in the x,T phase diagram; hence it may contain ordered crystallites. In any case, there seems to be a qualitative difference in the glass state between $x=0.20$ and 0.53.

An alternative definition of $\tilde{T}$ refers to the first appearance of the extra linewidth. This happens at temperatures ranging from 120 to 180 K, and the highest values are obtained for $x=0.65$ and 0.70. Following the reasoning from above, the first broadening is of dynamic origin. The temperature $\tilde{T}$ defined in this way gives the approximate temperature above which the center-of-mass lattice can no longer respond to the fast CN rotations. Thus there is some justification to call $\tilde{T}$ the freezing temperature characteristic for an x-ray experiment.

CONCLUSIONS

At low temperatures the mixed crystals show four elastically ordered phases which can be all derived from the cubic, high-temperature phase by the onset of spontaneous shear strains. In the glass state there is a distribution of shear strains. The low-temperature states, regardless of whether they are phases of long-range order or glasslike states, are announced by a broadening of the powder lines in the cubic phase.

A unified view of the low-temperature structures of the mixed crystals can be formulated in the following tentative way: Starting from pure KCN, lowering of the CN concentration leads to a reduction of the strength of the crystal field, and more isotropic distributions of the CN orientations, which, in turn, is connected by a further softening of the elastic shear constant C_{44}, as shown theoretically by Michel.[2] The first-order character of the transition to the elastically ordered state is progressively reduced. From recent neutron work,[16] we conclude that, finally, at $x=0.7$, the softening of C_{44} when approaching the phase transition is complete and the phase transition has become of second order. A strong increase of the mean-square displacements at T_c as postulated by theoretical work[14] has also been observed experimentally.[16] Formally, one could speak of a melting transition. A real crystal will, of course, avoid the divergence and remain in a state of finite strained blocks, a state that one might call a glass.

[1]F. Lüty, in *Defects in Insulating Crystals,* edited by V. M. Turkevich and K. K. Shvarts (Springer, Berlin, 1981), pp. 69–89.
[2]K. H. Michel, Z. Phys. **54**, 129 (1984).
[3]D. L. Price, J. M. Rowe, J. J. Rush, E. Prince, D. G. Hinks, and S. Susman, J. Chem. Phys. **56**, 3697 (1972).
[4]S. Haussühl, Solid State Commun. **13**, 147 (1973).
[5]C. W. Garland; J. Z. Kwiecien, and J. C. Damien, Phys. Rev. B **25**, 5818 (1982).
[6]J. M. Rowe, J. J. Rush, and S. Susman, Phys. Rev. B **28**, 3506 (1983).
[7]K. Knorr and A. Loidl, Z. Phys. B **46**, 219 (1982).
[8]S. Bhattacharya, S. R. Nagel, L. Fleishman, and S. Susman, Phys. Rev. Lett. **48**, 1267 (1982).
[9]R. Feile, A. Loidl, and K. Knorr, Phys. Rev. B **26**, 6875 (1982).
[10]K. H. Michel and J. M. Rowe, Phys. Rev. B **22**, 1417 (1980).
[11]A. Loidl, R. Feile, K. Knorr, and J. K. Kjems, Phys. Rev. B **29**, 6052 (1984).
[12]B. De Raedt, K. Binder, and K. H. Michel, J. Chem. Phys. **75**, 2977 (1981).
[13]S. Alexander and D. Amit, J. Phys. A **8**, 1988 (1975).
[14]R. Folk, H. Iro, and F. Schwabl, Z. Phys. B**25**, 69 (1976).
[15]J. M. Rowe, J. J. Rush, D. G. Hinks, and S. Susman, Phys. Rev. Lett. **43**, 1158 (1979).
[16]K. Knorr, A. Loidl, and J. K. Kjems (unpublished).